Supporting information:

Controlling processing, morphology and mechanical performance in blends of polylactide and thermotropic polyesters.

Gijs W. de Kort[1], *Sanjay Rastogi*[1], *Carolus H. R. M. Wilsens*[1,*]

[1]Aachen-Maastricht Institute of BioBased Materials (AMIBM), Maastricht University, P.O. Box 616, 6200MD, Maastricht, The Netherlands.

*Corresponding author: karel.wilsens@maastrichtuniversity.nl

Supporting Information: 12 pages, 2 Tables, 8 Figures.

Parameters for the critical capillary number ($\kappa_{critical}$).

The critical capillary number marks the conditions where a droplet in a flow field becomes instable and can break up. This value depends on the type of flow field. The parameters used to calculate $\kappa_{critical}$ were taken from literature (references 30 and 35 of the original manuscript) and are listed below.

Table S*1*: Constants for calculation of the critical capillary number for shear- and extensional flow fields.

Flow-field	c_1	c_2	c_3	c_4	c_5
Shear	-0.506	-0.0994	0.124	-0.115	-0.611
Extension	-0.6485	-0.02442	0.02221	-0.00056	-0.00645

$$\log(\kappa_{critical}) = c_1 + c_2 \cdot \log(\lambda) + c_3 \cdot \log(\lambda)^2 + \frac{c_4}{\log(\lambda) + c_5}$$

Time-temperature superposition of PLLA.

The relaxtion time of the PLLA melt at the processing temperatures was determined using time-temperature superposition. The obtained mastercurve and shift factors are reported.

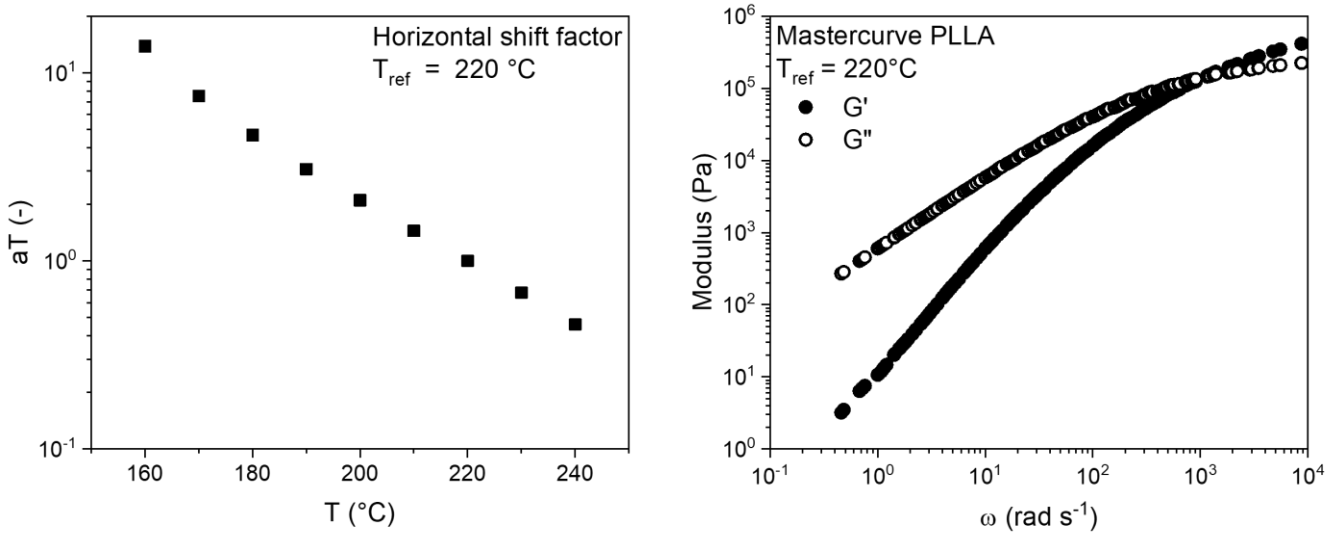

Figure S*1*: Horizontal shift factors (left) and mastercurve (right) obtained from time-temperature superposition of the PLLA (Corbion L130) used in this study at a reference temperature of 220 °C.

Analyses of POM images of the blends in the barrel.

In the injection molding process, the molten blend is extruded into a heated barrel prior to injection into the mold. The residence time in the barrel is typically 10 s to 1 min. During this stage of the process, the melt was not subjected to stresses, allowing stretched particles to relax. This process was mimicked by ex-situ heating the extrudate to the processing temperature. The resultant morphology was analyzed via POM, as the particles are easily distinguished upon dissolution of the PLLA matrix in a mixture of dichloromethane and acetone (ratio 3:1 by volume). The obtained images were processed and analyzed via ImageJ 1.50i. Several parameters describing the morphology are listed in Table S2, the obtained particles size distributions (by number and by cumulative volume) are supplied in Figure S2, and both original POM images and the processed images are shown in Figures S3 – S6.

Table S2: Morphological parameters of the blends during the barrel phase.

	d_{th} (µm)	d_{min} (µm)	d_{max} (µm)	d_{avg} (µm)	V_{avg} (µm^3)	c_{avg} (-)	N (-)
10 wt% LCP-A	0.19	0.7	10.4	2.9 ± 2.0	36.2 ± 75.0	0.75 ± 0.14	150
30 wt% LCP-A	0.19	0.6	28.7	3.0 ± 3.4	152 ± 1025	0.71 ± 0.16	193
10 wt% LCP-B	0.17	0.3	3.5	1.5 ± 0.7	2.8 ± 3.7	0.77 ± 0.16	223
30 wt% LCP-B	0.17	0.6	9.0	2.2 ± 1.3	12.8 ± 30.6	0.77 ± 0.14	484

d_{th}: theoretical minimum droplet diameter based on $\kappa = \kappa_{critical}$. The measured viscosities and assumptions for the interfacial tension and shear rate during extrusion (ν_{12} = 10 mN m^{-1} and γ = 100 s^{-1}) were used in the calculation.

d_{min}: minimal droplet diameter (based on area).

d_{max}: maximum droplet diameter (based on area).

d_{avg}: average droplet diameter (based on area).

V_{avg}: average droplet volume (based on area).

c_{avg}: average circularity of droplets, where 1.0 is indicative of a perfect circle and values approaching 0.0 represent elongated polygons. $circularity = 4\pi\ (area/perimeter^2)$

N: number of droplets observed in POM image

Analysis of POM images was carried out via ImageJ 1.50i (http://imagej.nih.gov/ij)

The images were converted to grayscale and subsequently a threshold was applied. The particles were analyzed via the 'Analyze Particles' function available in the software.

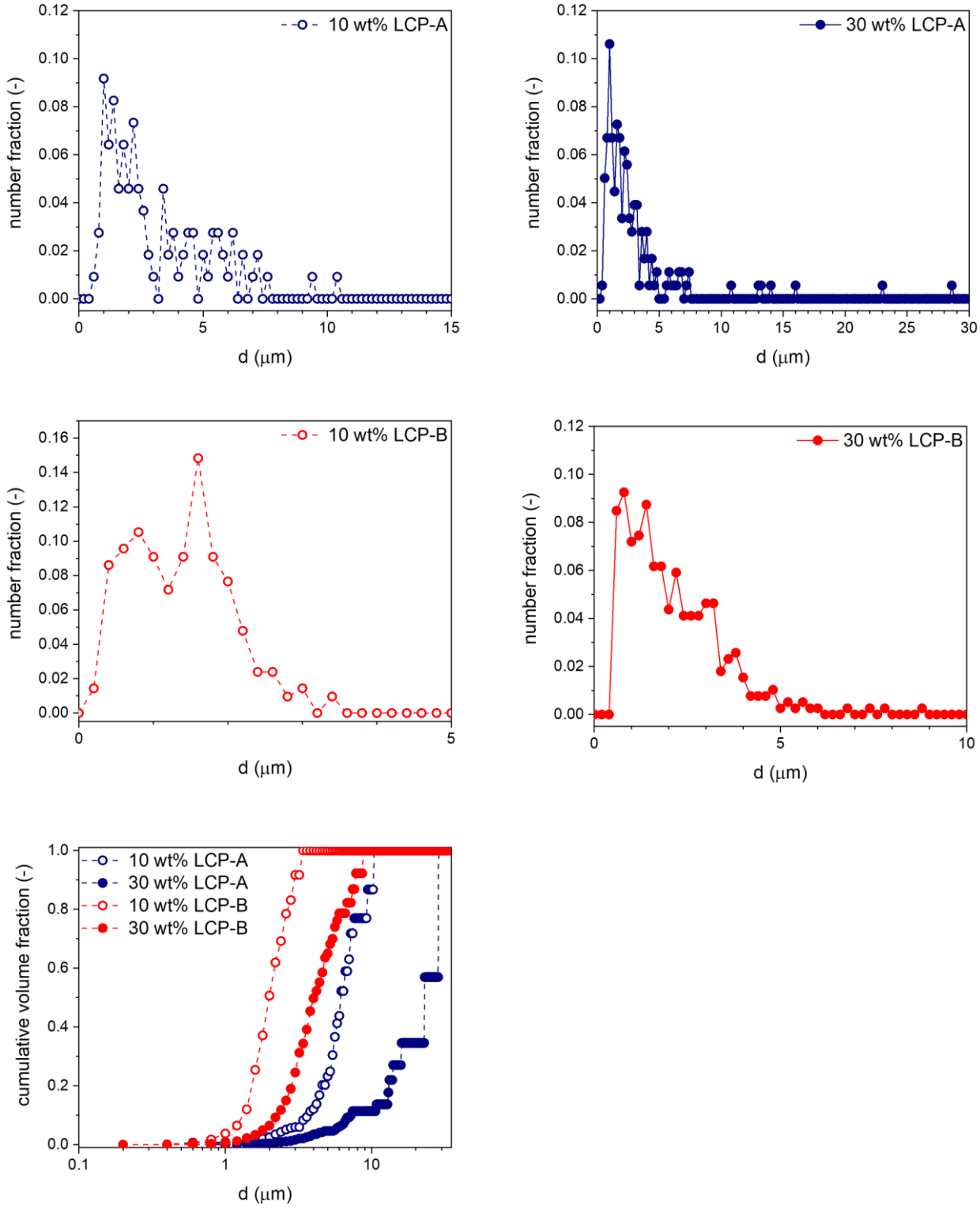

Figure S2: Particle size distributions by number of blends containting: 10 wt% LCP-A (top left), 30 wt% LCP-A (top right), 10 wt% LCP-B (middle left), and 30 wt% LCP-B (middle right). Cumulative particle volume distributions of all the blends (bottom).

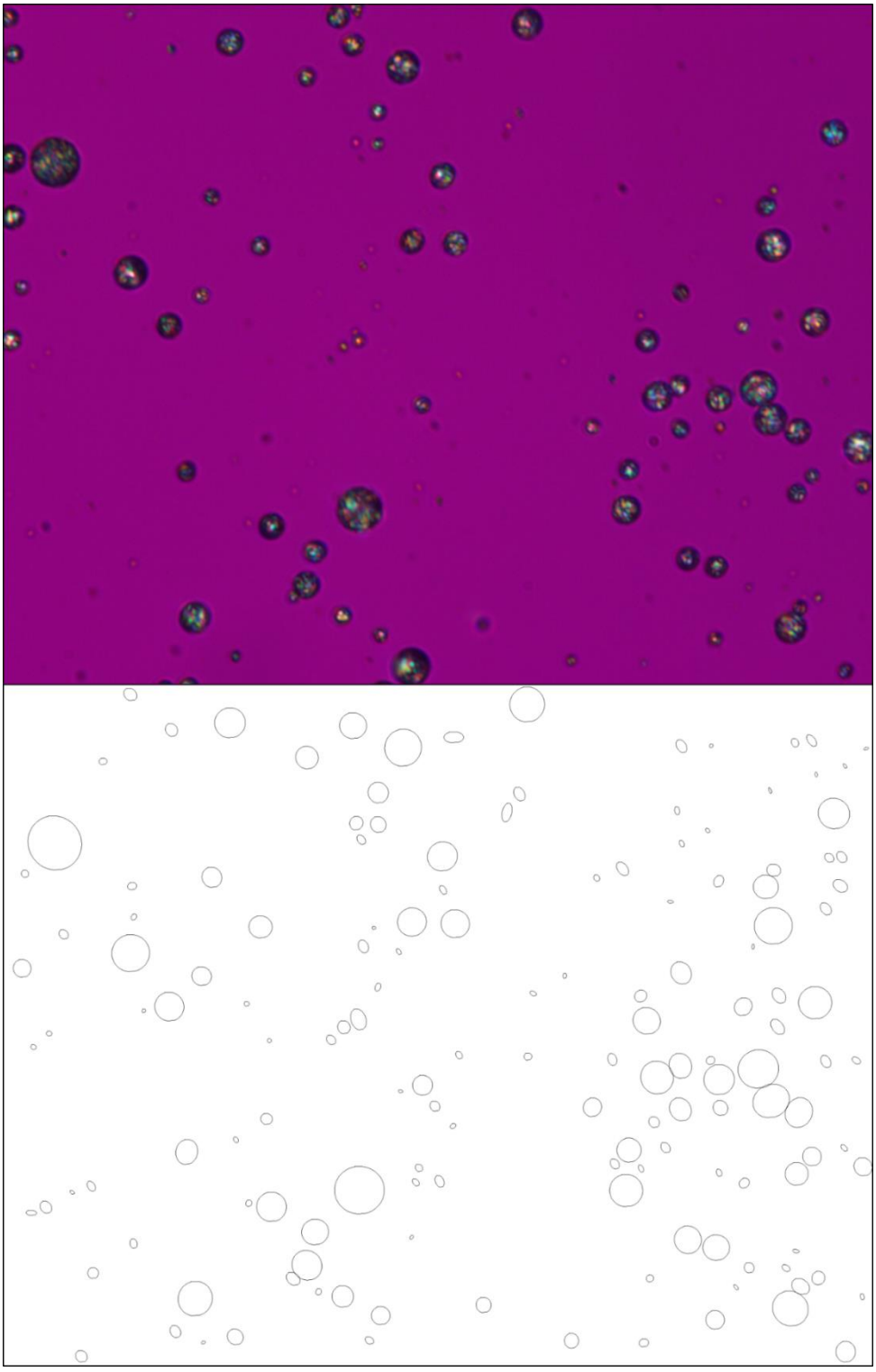

Figure S*3*: POM image (top) and processed image (bottom) of a blend containing 10 wt% LCP-A.

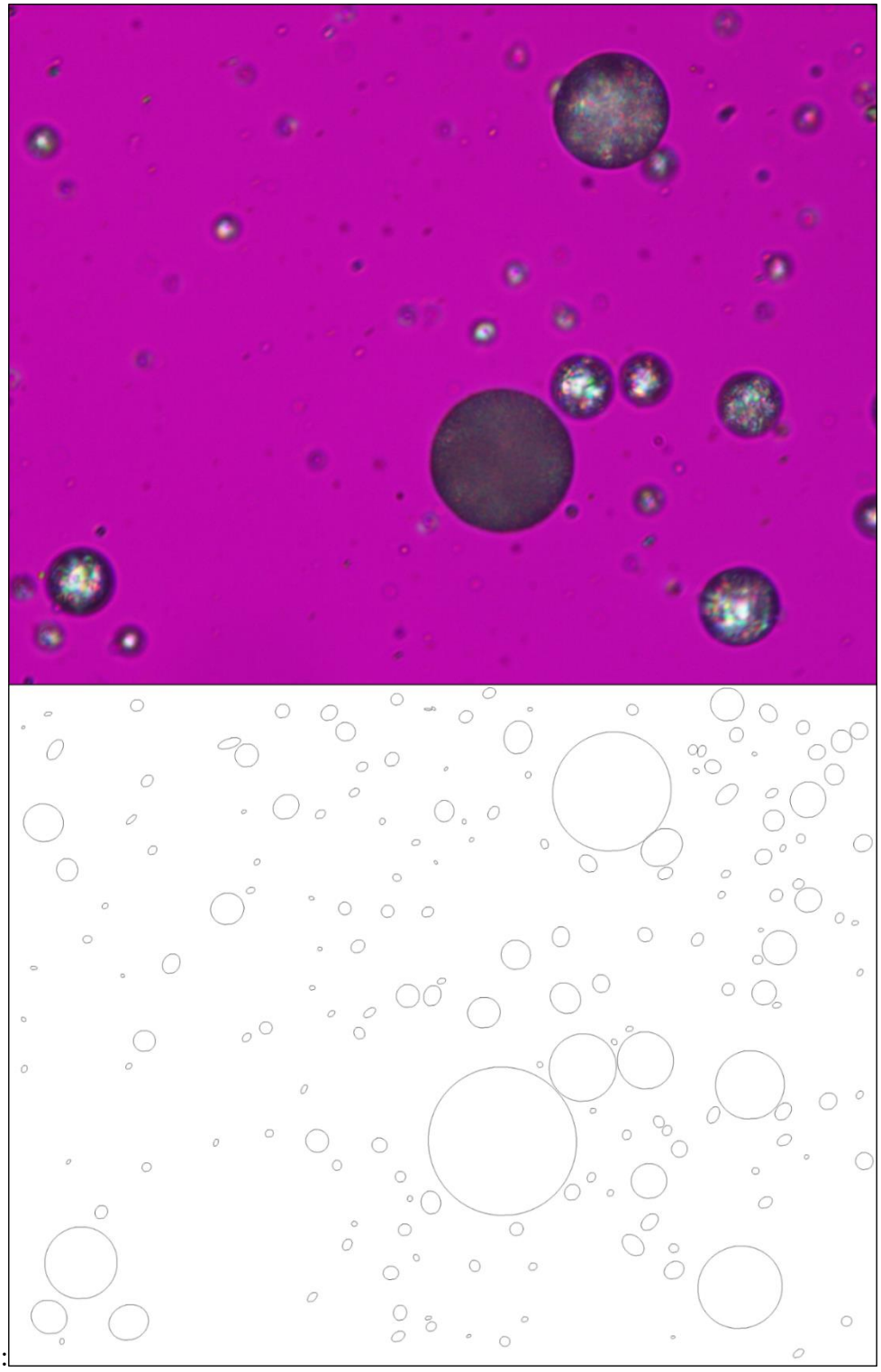

Figure S*4*: POM image (top) and processed image (bottom) of a blend containing 30 wt% LCP-A.

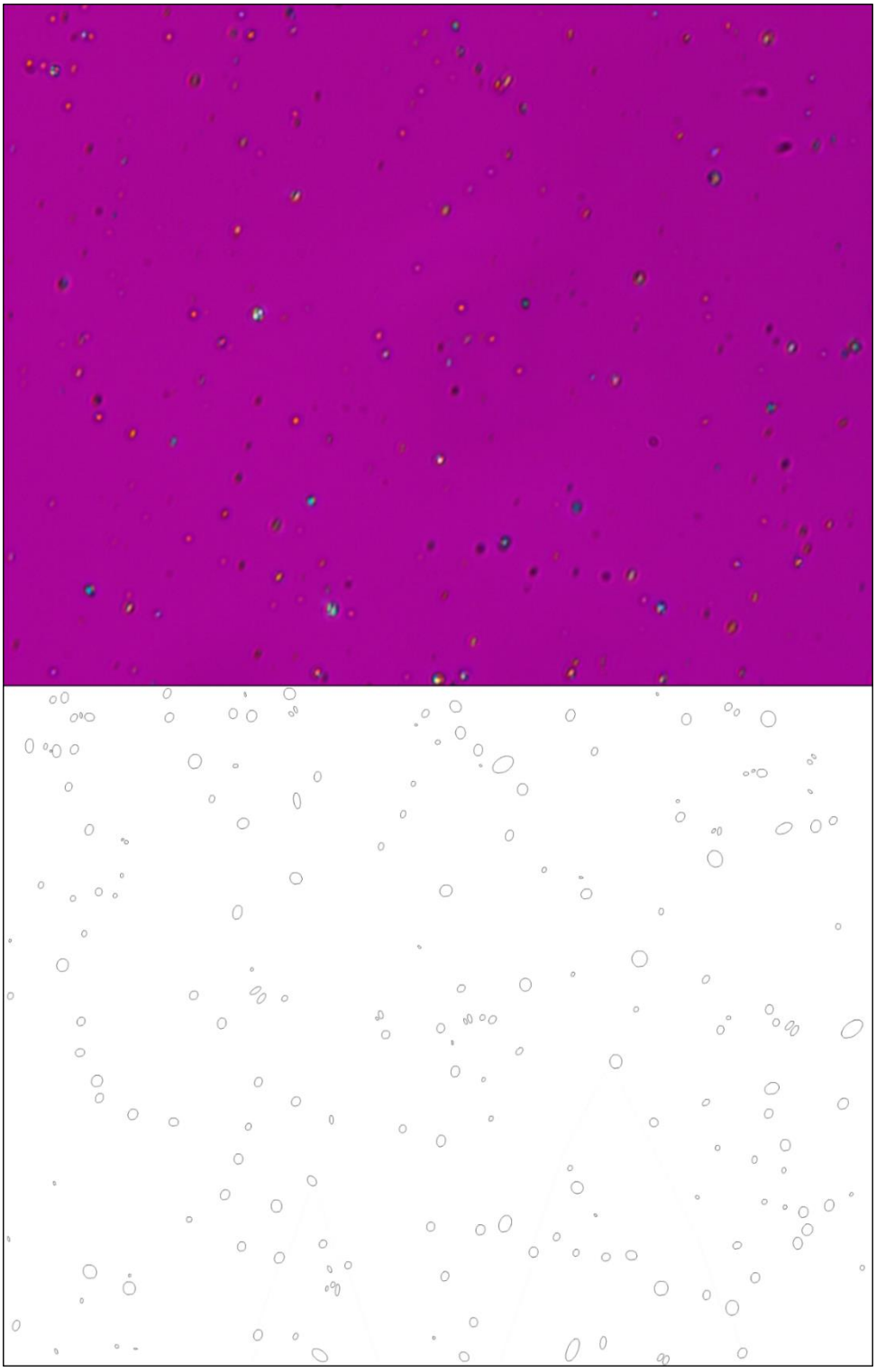

Figure S5: POM image (top) and processed image (bottom) of a blend containing 10 wt% LCP-B.

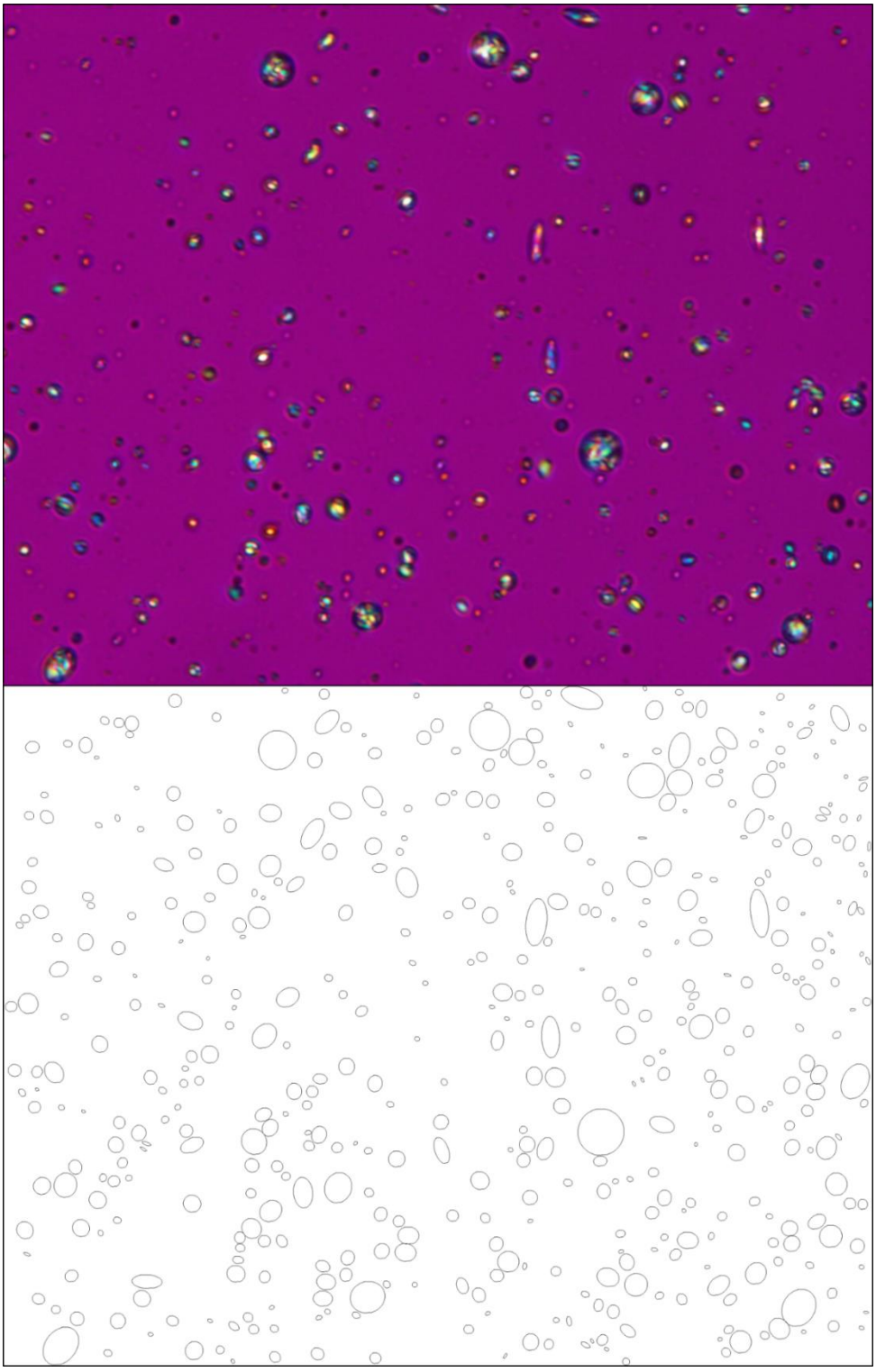

Figure S*6*: POM image (top) and processed image (bottom) of a blend containing 30 wt% LCP-B.

Microstructure of injection molded samples containing 10 wt% LCP.

Analogous to the injection molded samples containing 30 wt% LCP, the microstructure of the samples containing 10 wt% LCP were evaluated via SEM and WAXD (Figure S7)

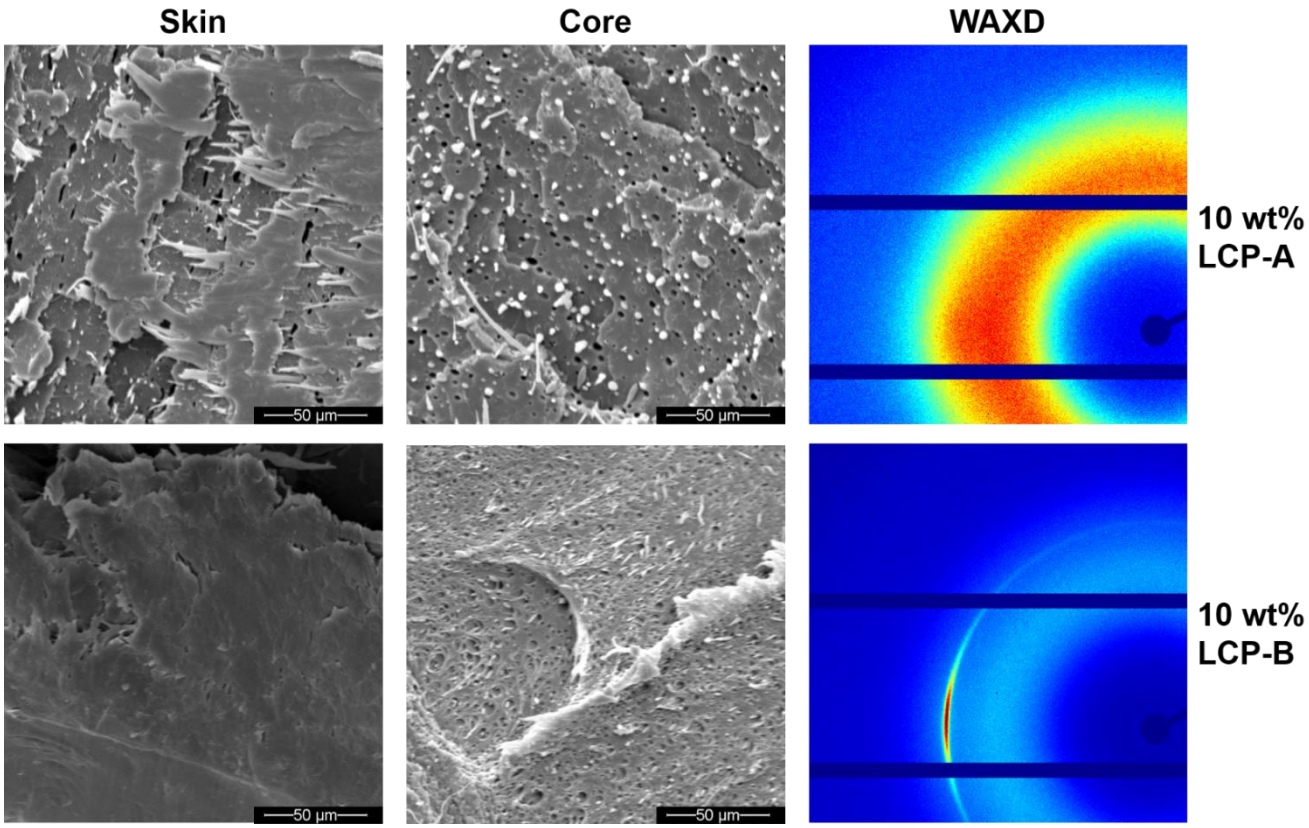

Figure S7: Microstructure of injection molded samples: SEM-images of sample skin (left, SEM-images of sample core (middle), and diffractograms (right).

Comparison of melt drawn and injection molded samples.

We stated that an extensional flow field is the most effective route to morphology consisting of LCP fibrils with a high degree of interchain orientation. This is illustrated by the diffractograms shown in Figure S8. The LCP signal in the melt drawn tapes, in comparison to the injection molded samples, is more narrow and more intense with respect to the amorphous halo of the PLLA, indicating a higher degree of interchain orientation. Additionally, the diffractograms of the 30 wt% LCP-B/PLLA blend show a signal corresponding to isotropic LCP crystallites for the injection molded sample, whereas this signal is absent in the melt drawn tape.

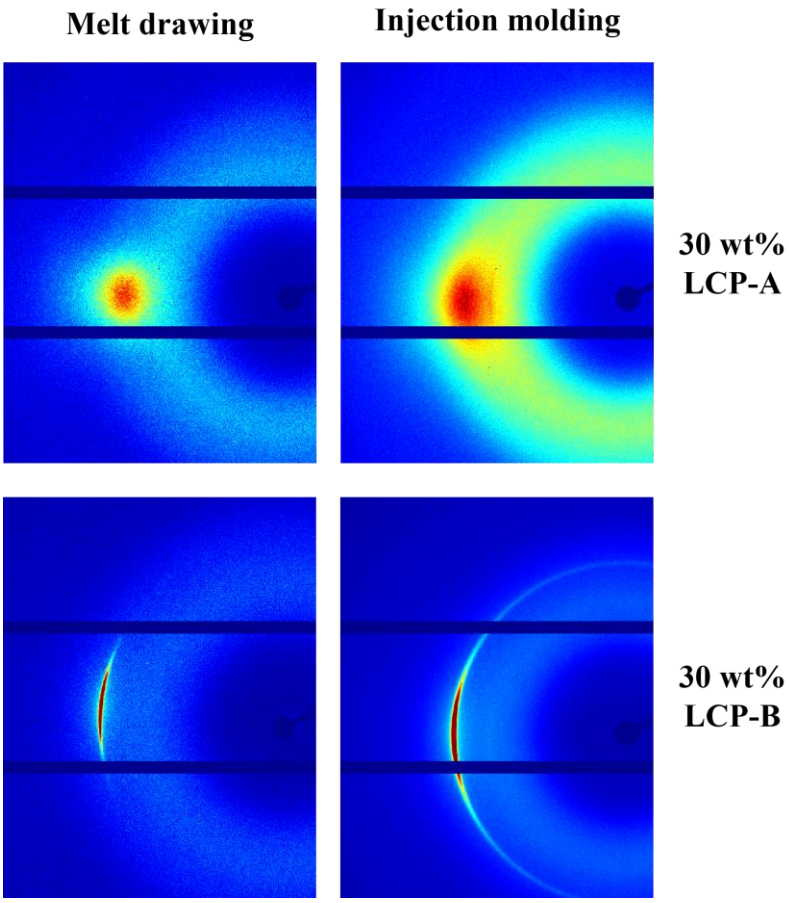

Figure S*8*: Diffractograms comparing the microstructure of melt drawn and injection molded LCP/PLLA composites containing 30 wt% LCP.